

Anti-Jahn-Teller Polaron

Philip B. Allen and Vassili Perebeinos

Department of Physics and Astronomy, State University of New York, Stony Brook, New York 11794-3800

(October 24, 2019)

Distortions of the oxygen sublattice couple to e_g orbitals of Mn^{3+} and drive an $E \times e$ cooperative Jahn-Teller (orbital ordering) transition in LaMnO_3 . A simple model for this transition is studied. Without further adjustment, the model gives simple predictions about the shape and stability of the small (anti-Jahn-Teller) polarons which form when holes are doped into the material, and a new description of the lightly doped insulator, the anti-ferromagnetic to ferromagnetic transition, and the metal-insulator transition.

71.38.+i,71.30.+h,75.30.Vn

I. INTRODUCTION

The doped manganites $\text{Re}_{1-x}\text{A}_x\text{MnO}_3$ (where Re is typically La and A is typically Sr or Ca) have a fascinating (T, x) (temperature, concentration) phase diagram, including “colossal magnetoresistance” [1] when $T \approx 250\text{K}$ and $x \approx 0.20$. Experiment (transport [2], optical [3], diffraction [4], EXAFS [5], isotope studies [6]) and theory [7] indicate the appearance of polarons at this point in (T, x) . It is less well appreciated that small polarons are essential to explain the insulating phase at smaller x and $0\text{K} < T < 750\text{K}$ [8]. We study a simple model for the cooperative Jahn-Teller (JT) transition, and use the model to predict properties of small polarons in lightly-doped material, including how they affect magnetic order and the metal-insulator transition. By working in the limit of large on-site Coulomb repulsion U , we find that properties of the polaron are simple enough to describe analytically, with small perturbative corrections.

There is disagreement over the relative role of Coulomb, magnetic, and electron-phonon effects. We offer a simple unified picture in which the relevant energy scales in descending order are: (1) Coulomb interactions are inactive after establishing the dominant Hubbard and Hund energy scales; (2) electron-phonon interactions drive orbital ordering by the JT mechanism; (3) when doped, electron-phonon interactions via orbital ordering give small anti-JT polarons; and finally (4) orbital ordering disrupted by polarons is responsible for the unusual sequence of magnetic phases.

A canonical “Jahn-Teller polaron” [9] is the excess electron in BaTiO_3 [10], which sits in a triply degenerate t_{2g} level. A local distortion of the lattice splits the degenerate levels. Beyond a critical coupling strength, this lowers the energy and traps the electron in a small polaron state.

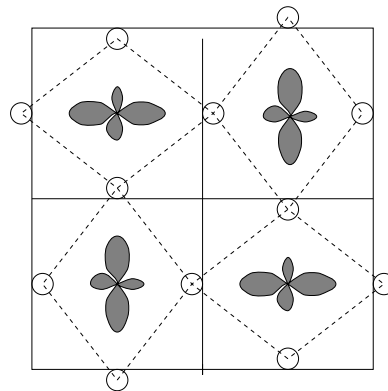


FIG. 1. Base plane (x-y plane) of Jahn-Teller distorted LaMnO_3 . Rotations of oxygen octahedra are omitted, and distortions are exaggerated. Oxygens are displaced only along Mn-O-Mn bonds.

By contrast, the polarons in LaMnO_3 are “anti-JT polarons.” When pure, the valence is Mn^{3+} , with d^4 configuration in the high-spin state $t_{2g}^3 e_g^1$ with the doubly-degenerate e_g level singly occupied. Below the JT structural transition at $T_s=750\text{K}$ [11], oxygen octahedra distort as illustrated schematically in Fig. 1, lifting the e_g degeneracy and lowering the energy of the occupied orbitals. When a hole is added, we show that a small polaron is formed by locally “undoing” [8] the JT distortion, pinning the hole onto a Mn^{4+} site with a filled t_{2g} shell. The model Hamiltonian is $\mathcal{H} = \mathcal{H}_t + \mathcal{H}_{\text{ep}} + \mathcal{H}_L + \mathcal{H}_U$.

$$\mathcal{H}_t = t \sum_{\ell, \pm} \{ [c_x^\dagger(\ell) c_x(\ell \pm \hat{x}) + \text{H.C.}] + [x \rightarrow y] + [y \rightarrow z] \} \quad (1)$$

$$\mathcal{H}_{\text{ep}} = -\frac{4g}{\sqrt{3}} \sum_{\ell} \{ [c_x^\dagger(\ell) c_x(\ell) Q_x(\ell)] + [x \rightarrow y] + [y \rightarrow z] \} \quad (2)$$

$$\mathcal{H}_L = \frac{K}{2} \sum_{\ell} [u_x(\ell + \frac{1}{2}\hat{x})^2 + u_y(\ell + \frac{1}{2}\hat{y})^2 + u_z(\ell + \frac{1}{2}\hat{z})^2] \quad (3)$$

$$\mathcal{H}_U = U \sum_{\ell} c_2^\dagger(\ell) c_2(\ell) c_3^\dagger(\ell) c_3(\ell) \quad (4)$$

The c^\dagger operators create electrons whose spins (because of the large Hund’s rule energy) are parallel to the $S=3/2$

core spin, and hopping only operates between adjacent Mn sites with parallel spins. We use as a simplifying device an overcomplete basis for the two-dimensional e_g manifolds, with orbitals $\psi_x = 3x^2 - r^2$, $\psi_y = 3y^2 - r^2$, and $\psi_z = 3z^2 - r^2$, each pointing along one of the Cartesian axes, and hopping only along that direction. After re-expressing \mathcal{H}_t in terms of the orthogonal orbitals $\psi_2 \propto x^2 - y^2$ and $\psi_3 \propto 3z^2 - r^2$, it turns out to be the correct nearest-neighbor two-center Slater-Koster [12] model, with $t = (dd\sigma)$, $(dd\pi)$ not entering due to symmetry, and $(dd\delta) = 0$. H.C. stands for Hermitean conjugate.

The only lattice degree of freedom is oxygen motion along the direction of the bonds to the nearest two Mn atoms, with a harmonic restoring force $-Ku_x$. Variables $Q_x(\ell) = u_x(\ell + \frac{1}{2}x) - u_x(\ell - \frac{1}{2}x)$ measure the local expansion of oxygens on the x -axis around the ℓ -th Mn atom. This expansion lowers the energy ϵ_x of orbital ψ_x by $\partial\epsilon_x/\partial Q_x = -4g/\sqrt{3}$. We work in adiabatic approximation (oxygen mass = ∞ .) This model generalizes to e_g electrons the model of Rice and Sneddon [13] for s electrons in BaBiO₃. The same model, but with longer range forces, was used by Millis [14] for LaMnO₃.

The electron-phonon term in the Hamiltonian (2) is conveniently split into Jahn-Teller and breathing parts, $\mathcal{H}_{\text{ep}} = \mathcal{H}_{\text{JT}} + \mathcal{H}_{\text{br}}$:

$$\mathcal{H}_{\text{JT}} = -g \sum_{\ell} \begin{pmatrix} c_2^{\dagger}(\ell) & c_3^{\dagger}(\ell) \end{pmatrix} \begin{pmatrix} -Q_3(\ell) & -Q_2(\ell) \\ -Q_2(\ell) & Q_3(\ell) \end{pmatrix} \begin{pmatrix} c_2(\ell) \\ c_3(\ell) \end{pmatrix} \quad (5)$$

$$\mathcal{H}_{\text{br}} = -\sqrt{2}(1 + \beta)g \sum_{\ell} Q_1(\ell) [c_2^{\dagger}(\ell)c_2(\ell) + c_3^{\dagger}(\ell)c_3(\ell)] \quad (6)$$

where the breathing amplitude is $Q_1 = \sqrt{2/3}(Q_x + Q_y + Q_z)$, Q_2 is $Q_x - Q_y$, and Q_3 is $(2Q_z - Q_x - Q_y)/\sqrt{3}$, in standard Van Vleck [15] notation. A non-zero β was introduced by Millis, to represent additional charge coupling to the breathing mode. To simplify the model, we set β to zero in the following.

We have solved this Hamiltonian for doping $x = 0$ in two opposite limits, U/t small, by a Hartree-Fock calculation, and U/t infinite. A distortion $(Q_2, Q_3) = Q(\cos\theta, \sin\theta) \exp(i\vec{q} \cdot \vec{\ell})$ is introduced. We minimize elastic and electron energy to find optimal distortion parameters Q, θ , and \vec{q} . The two limits give similar answers. The optimal distortion has wavevector $\vec{q} = (\pi, \pi, \pi)$. Unless we add anharmonic or strain terms to select more strongly a direction in (Q_2, Q_3) -space, the energy depends only weakly on θ in HF approximation, and not at all on θ in $U \rightarrow \infty$ approximation. Rather than introduce new parameters, we select the observed Q_2 -type distortion ($\theta = 0$).

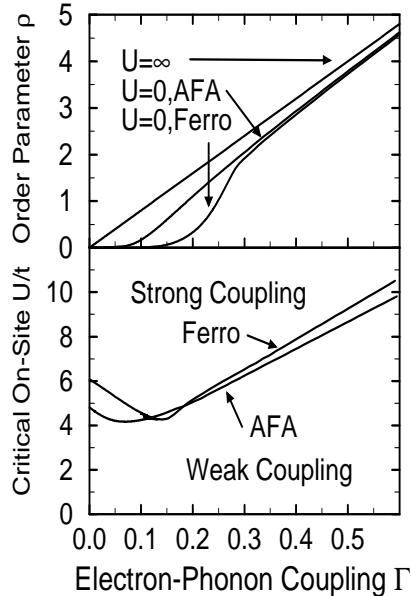


FIG. 2. Critical value of on-site repulsion U which separates weakly from strongly-correlated solutions. The upper panel shows the Jahn-Teller distortion $\rho = gu/t$ as a function of $\Gamma = g^2/Kt$ for weak and strong-coupling solutions.

For LaMnO₃, we estimate the parameters to be $t \approx 0.5$ eV and $U \approx 6$ eV. Electron-phonon effects enter through the dimensionless parameter Γ which we estimate to be ≈ 0.25 . The lower panel of Fig. 2 shows that for these choices, the $U \rightarrow \infty$ approximation is better. The upper panel shows that the JT distortion does not depend much on U for $\Gamma \geq 0.25$.

It is convenient to make a 45° rotation in (ψ_2, ψ_3) -space, to a new orthogonal basis,

$$\psi_X = \frac{1}{\sqrt{2}}(\psi_2 - \psi_3) = \alpha\psi_x - \beta\psi_y - \gamma\psi_z \quad (7)$$

$$\psi_Y = -\frac{1}{\sqrt{2}}(\psi_2 + \psi_3) = -\beta\psi_x + \alpha\psi_y - \gamma\psi_z \quad (8)$$

where $(\alpha^2, \beta^2, \gamma^2) = (1.21, .09, .67)$. The orbitals ψ_X and ψ_Y point strongly in the \hat{x} and \hat{y} directions, and are equivalent under a 90° rotation in real space, as shown in Fig. 1. The ground electronic state with perfect orbital order is

$$|G\rangle = \prod_{\ell}^A c_X^{\dagger}(\ell) \prod_{\ell'}^B c_Y^{\dagger}(\ell') |0\rangle, \quad (9)$$

where A and B label sublattices where the phase of the orbital order $\exp(i\vec{q} \cdot \vec{\ell})$ is ± 1 respectively. The energy $\langle G | \mathcal{H} | G \rangle = -NgQ + NKQ^2/16$ has minimum value $E/N = -4\Gamma t$ at $Q = 8g/K$ as shown on Fig. 2. This JT phase is insulating; the gap to charge excitations (U) is large, but orbital excitations require only energy $16\Gamma t \approx 2$ eV, and spin excitations occur down to low energies, with characteristic energy $J \approx t^2/U \approx 500$ K. As

argued by Goodenough [11], the source of the ferromagnetic in-plane exchange ($J_1 S^2 = 3.32$ meV [16]) is orbital order which favors virtual hops from filled A sublattice ψ_X orbitals to empty B sublattice ψ_X with spin parallel to avoid a Hund penalty. When orbitals are not ordered, the Hund penalty is outweighed by the multiplicity of anti-parallel spin hops; the c-axis exchange is of this type, with $J_2 S^2 = -2.32$ meV.

What happens when a hole is added? It can go into any of the states $|\ell A\rangle$ and $|\ell' B\rangle$ which are occupied in Eqn. 9. When $\Gamma = 0$ the hole is free to hop among these states, no matter how large is U , since spins are aligned in the planes. When $\Gamma > 0$ it costs energy $gQ = 8\Gamma t$ in lost JT energy to remove the electron. There are two different ways to regain some energy. **(a)** The hole can delocalize, forming a Bloch state. There is a band with energy $\epsilon_k/t = (1/2)(\cos k_x + \cos k_y)$ plus an additional term $-\cos k_z$ in the Ferro case. The minimum energy of the delocalized hole is $E_{h,ext}/t = 8\Gamma - 1$ (AFA) and $8\Gamma - 2$ (Ferro). **(b)** If the distortions Q_ℓ are locally readjusted, a bound state can be formed, which will be non-metallic because a small impurity potential will pin it. In first approximation, put the hole at a single A site. The nearest \hat{x} -oxygens, instead of being displaced outwards by $u = 2g/K$, should now displace inwards by $u = -(\sqrt{4/3} - 1)g/K$; the \hat{y} -oxygens, formerly displaced inwards by $u = -2g/K$, now displace slightly further inwards, by $u = -(\sqrt{4/3} + 1)g/K$; the \hat{z} -neighbors, formerly undisplaced, now displace in by $u = -\sqrt{4/3}g/K$. The pattern of this anti-JT polaron is shown in Fig. 3. The energy $E_{h,pol}/t$ needed to make the hole is reduced from 8Γ in lost JT energy to 2Γ . This energy comes partly from a reduction in the strain cost and partly from energy of breathing. Setting $E_{h,ext} = E_{h,pol}$, we conclude that small polarons are stable for $\Gamma > 1/6$ in AFA phase, and that ferromagnetism, by enhancing the delocalization energy, prevents small polarons until $\Gamma > 1/3$.

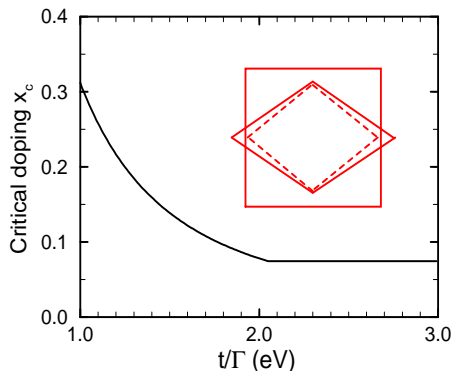


FIG. 3. Critical concentration x_c for the AFA to Ferro transition as a function of coupling constants t/Γ . The inset shows (in exaggerated form) the shape of Anti-Jahn-Teller polaron (dashed lines) in the x-y plane. The relative positions of O atoms (at vertices of rhombus) in the pure JT (solid line) state and in the polaron state are accurate.

The three largest errors in the calculation of the hole energy are (1) the localized hole can spread somewhat onto neighboring Mn atoms; (2) the Hilbert space for both localized and delocalized hole wavefunctions should include states with orbital defects (sites occupied singly, but by the orbital of wrong orientation); (3) a hole in AFA phase will lower its energy further by causing spin canting on Mn atoms in adjacent planes, thus permitting interplanar hopping, and eventually driving an AFA to Ferro transition.

We have calculated these effects by perturbation theory. The probability that a small hole polaron will be found away from the central site is $a/(1.0366 + a)$ where $a = 0.0059/\Gamma^2$ (AFA) and $0.0099/\Gamma^2$ (Ferro). At the smallest Γ where small polarons are stable, the probability is 19% and 10%. This shows that the small polaron is very well localized. The first two effects cause the energy to be lowered by $Ct\Gamma + C't/\Gamma$ with $C=0$ for delocalized states and 0.49 for localized states, and $C'=(0.11, 0.14)$ in (Ferro, AFA) delocalized states and (0.11, 0.17) for delocalized. The shifts are small for values of $\Gamma \geq 0.2$. The critical value of Γ for small polaron formation changes from $\Gamma_c = 1/6$ to 0.157 (AFA) and from $1/3$ to 0.294 (Ferro).

Effect (3), the spin-canting problem, has usually been discussed on the assumption that holes are delocalized [19]. Treating spins classically, the additional delocalization energy gained when adjacent layers realign from 180° to $180^\circ - \theta$ is $t \sin(\theta/2)$ per hole; the exchange cost of realignment is $J_2 S^2 (1 - \cos(\theta))$ per Mn atom. The optimum canting angle is $\sin(\theta/2) = xt/4|J_2|S^2$, which gives a small critical concentration $x_c = 4|J_2|S^2/t$ for complete rotation to the Ferro phase. Localized holes tilt spins on only near-neighbor Mn atoms in adjacent planes, gaining less hopping energy than delocalized holes because the electron hops into an anti-JT-distorted hole site. The energy gain is $(39/640)(t/\Gamma) \sin(\theta/2)$. If we neglect the rotation of any except first-neighbor spins, the magnetic energy loss around the localized hole is $(8J_1 + 2|J_2|)S^2(1 - \cos(\theta))$ per hole, giving the optimum local rotation $\sin(\theta/2) = 0.49(eV^{-1})t/\Gamma$. For $t > 2.04\Gamma$ eV, the adjacent spins are completely flipped. Comparing the magnetic energy loss per spin with the energy loss of the Ferro state, we find a critical concentration plotted in Fig. 3. Experimentally the AFA/Ferro phase boundary occurs at $x_c=0.08$ for Sr-doped LaMnO_3 [20] and at $x_c=0.15$ for Ca doping [21]. These values are easily reconciled with the localized hole picture, but demand rather too small a value of t in the delocalized picture. The smaller Ca ion causes larger Mn-O-Mn bond angles which results in a smaller t and a larger x_c .

Numerous effects are left out of the model. Macroscopic strain, tilting of oxygen octahedra, and additional zero-point magnetic and non-adiabatic lattice fluctuations all could be added and would affect the $T = 0$ properties discussed here, but we believe that the effects we did include are the most important ones. A $T > 0$ treatment of all these effects is a bigger challenge. Per-

haps more interesting would be an extension of the $T = 0$ calculations to higher doping where a remarkable variety of textured phases is being unravelled [22]. The properties of LaMnO₃-related materials are incredibly rich, yet surprisingly understandable, in contrast to certain other transition-metal oxide systems.

ACKNOWLEDGMENTS

We thank W. Bao, M. Blume, D. E. Cox, J. P. Franck, J. B. Goodenough, J. P. Hill, D. I. Khomskii, and J.-S. Zhou for helpful conversations, and V. N. Kostur for the inspiration to start the project. This work was supported in part by NSF grant no. DMR-9725037.

-
- [1] G. Jonker and J. H. van Santen, *Physica (Amsterdam)* **16**, 337 (1950); C.N.R. Rao and B. Raveau, editors, *Colossal Magnetoresistance, Charge Ordering, and Related Properties of Manganese Oxides*, World Scientific, Singapore, 1998.
- [2] M. Jaime, M. B. Salamon, M. Rubinstein, R. E. Treece, J. S. Horowitz, and D. B. Chrisey, *Phys. Rev. B* **54**, 11914 (1996); T. T. M. Palstra, A. P. Ramirez, S-W. Cheong, B. R. Zegarski, P. Schiffer, and J. Zaanen, *Phys. Rev. B* **56**, 5104 (1997); J. L. Cohn, J. J. Neumeier, C. P. Popoviciu, K. J. McClellan, and Th. Leventouri, *Phys. Rev. B* **56**, R8495 (1997); D. C. Worledge, L. Miéville, and T. H. Geballe, *Phys. Rev. B* **57**, 15267 (1998); J. P. Franck (private communication).
- [3] Y. Okimoto, T. Katsufuji, T. Ishikawa, A. Urushibara, T. Arima, and Y. Tokura, *Phys. Rev. Letters* **75**, 109 (1995); K. H. Kim, J. H. Jung, and T. W. Noh, *Phys. Rev. Letters* **81**, 1517 (1998); M. Quijada, J. Černe, J. R. Simpson, H. D. Drew, K. H. Ahn, A. J. Millis, R. Shrekala, R. Ramesh, M. Rajeswari, and T. Venkatesan, *cpmd-mat/9803201*.
- [4] S. L. Billinge, R. G. DiFrancesco, G. H. Kwei, J. J. Neumeier, and J. D. Thompson, *Phys. Rev. Letters* **77**, 715 (1996); D. Louca, T. Egami, E. L. Brosha, H. Röder, and A. R. Bishop, *Phys. Rev. B* **56**, 8475 (1997).
- [5] T. A. Tyson, J. Mustre de Leon, S. D. Conradson, A. R. Bishop, J. J. Neumeier, H. Röder, and J. Zang, *Phys. Rev. B* **53**, 13985 (1996); A. Lanzara, N. L. Saini, M. Brunelli, F. Natali, A. Bianconi, P. G. Radaelli, and S-W. Cheong, *Phys. Rev. Letters* **81**, 878 (1998).
- [6] G.-m. Zhao, K. Conder, H. Keller, and K. A. Müller, *Nature* **381**, 676 (1996).
- [7] A. J. Millis, P. B. Littlewood, and B. I. Shraiman, *Phys. Rev. Letters* **74**, 5144 (1995); A. J. Millis, B. I. Shraiman, and R. Mueller, *Phys. Rev. Letters* **77**, 175 (1996); A. J. Millis, R. Mueller, and B. I. Shraiman, *Phys. Rev. B* **54**, 5389 and 5405 (1996); H. Röder, J. Zang, and A. R. Bishop, *Phys. Rev. Letters* **76**, 1356 (1996); J. D. Lee and B. I. Min, *Phys. Rev. B* **55**, 12454 (1997).
- [8] Y. Yamada, O. Hino, S. Nohdo, R. Kanao, T. Inami, and S. Katano, *Phys. Rev. Letters* **77**, 904 (1996).
- [9] K. H. Höck, H. Nickisch, and H. Thomas, *Helv. Phys. Acta* **56**, 237 (1983).
- [10] S. Köhne, O. F. Schirmer, H. Hesse, T. W. Kool, and V. Vikhnin, *J. Superconductivity* (in press).
- [11] J. B. Goodenough, A. Wold, R. J. Arnott, and N. Menyuk, *Phys. Rev.* **124**, 373 (1961); J. Rodriguez-Carvajal, M. Hennion, F. Moussa, A. H. Moudden, L. Pinsard, and A. Revcolevschi, *Phys. Rev. B* **57**, 3189 (1998); Y. Murakami, J. P. Hill, D. Gibbs, M. Blume, I. Koyama, M. Tanaka, H. Kawata, T. Arima, Y. Tokura, K. Hirota, and Y. Endoh, *Phys. Rev. Lett.* **81**, 582 (1998).
- [12] J. C. Slater and G. F. Koster, *Phys. Rev.* **94**, 1498 (1954).
- [13] T. M. Rice and L. Sneddon, *Phys. Rev. Letters* **47**, 689 (1982).
- [14] A. J. Millis, *Phys. Rev. B* **53**, 8434 (1996).
- [15] J. H. Van Vleck, *J. Chem. Phys.* **7**, 72 (1939); J. Kanamori, *J. Appl. Phys.* **31**, 14S (1960); J. B. Goodenough, *Magnetism and the Chemical Bond*, Wiley Interscience, New York, 1963; p.202ff; K. I. Kugel and D. I. Khomskii, *Sov. Phys. JETP* **37**, 725 (1973).
- [16] F. Moussa, M. Hennion, J. Rodriguez-Carvajal, H. Moudden, L. Pinsard, and A. Revcolevschi, *Phys. Rev. B* **54**, 15149 (1996).
- [17] J. Yu, X.-Y. Chen, and W. P. Su, *Phys. Rev. B* **41**, 344 (1990).
- [18] P. B. Allen and V. N. Kostur, *Z. Phys. B* **104**, 605-612 (1997).
- [19] P. G. de Gennes, *Phys. Rev.* **118**, 141 (1960).
- [20] H. Kawano, R. Kajimoto, M. Kubota, and H. Yoshizawa, *Phys. Rev. B* **53**, 2202 (1996).
- [21] E. O. Wollan and W. C. Koehler, *Phys. Rev.* **100**, 545 (1955).
- [22] W. Bao, J. D. Axe, C. H. Chen, and S.-W. Cheong, *Phys. Rev. Letters* **78**, 543 (1997); P. G. Radaelli, D. E. Cox, M. Marezio, and S.-W. Cheong, *Phys. Rev. B* **55**, 3015 (1997); H. Kuwahara, Y. Moritomo, Y. Tomioka, A. Asamitsu, M. Kasai, R. Kumai, and Y. Tokura, *Phys. Rev. B* **56**, 9386 (1997); S. Mori, C. H. Chen, and S.-W. Cheong, *Nature* **392**, 473 (1998).